

Synthesis, X-ray Powder Structure, and Magnetic Properties of the New, Weak Ferromagnet Iron(II) Phenylphosphonate

Carlo Bellitto* and Fulvio Federici

CNR—Istituto di Chimica dei Materiali, Area della Ricerca di Montelibretti, Via Salaria Km. 29.5, C.P.10, I-00016 Monterotondo Staz., Roma, Italy

Angela Altomare* and Rosanna Rizzi

CNR—Istituto di Ricerca per lo Sviluppo di Metodologie Cristallografiche, c/o Dipartimento Geomineralogico, Università di Bari, Via Orabona 4, Campus Universitario, I-70125 Bari, Italy

Said A. Ibrahim

Department of Chemistry, Faculty of Science, Assiut University, Assiut, Egypt

Received December 29, 1999

A new molecule-based weak ferromagnet of formula $\text{Fe}[\text{C}_6\text{H}_5\text{PO}_3]\cdot\text{H}_2\text{O}$ was synthesized. It was characterized by thermogravimetric analysis and UV–visible and infrared spectroscopy, and the magnetic properties were studied using a superconducting quantum interference device magnetometer. The crystal structure of the compound was determined “ab initio” from X-ray powder diffraction data and refined by the Rietveld method. The crystals of $\text{Fe}[\text{C}_6\text{H}_5\text{PO}_3]\cdot\text{H}_2\text{O}$ are orthorhombic, space group $Pmn2_1$, with $a = 5.668(8)$ Å, $b = 14.453(2)$ Å, $c = 4.893(7)$ Å, and $Z = 2$. The title compound is isostructural with the previously reported lamellar $\text{M}[\text{C}_6\text{H}_5\text{PO}_3]\cdot\text{H}_2\text{O}$, $\text{M} = \text{Mn(II)}$, Zn(II) , and Cd(II) . The inorganic layers are made of Fe(II) ions octahedrally coordinated by five phosphonate oxygen atoms and one from oxygen of the water molecule. These layers are then separated by bilayers of the phenyl groups, and van der Waals contacts are established between them. The refinement has shown that the phenyl rings are disordered in the lattice. The oxidation state of the metal ion is +2, and the electronic configuration is d^6 ($S = 2$) high-spin, as determined from dc magnetic susceptibility measurements from 150 K to room temperature. Below 100 K, the magnetic moment of $\text{Fe}[\text{C}_6\text{H}_5\text{PO}_3]\cdot\text{H}_2\text{O}$ rises rapidly to a maximum at $T_N = 21.5$ K, and then it decreases again. The peak at T_N is associated with the 3D antiferromagnetic long-range ordering. Below the critical temperature, the title compound behaves as a “weak” ferromagnet, which represents the third type of magnetic materials characterized by having a finite zero-field magnetization, ferromagnets and ferrimagnets being the other two types. The large coercive field (i.e., 6400 G) observed in the hysteresis loop at $T = 10$ K is rare in molecule-based materials; it can be ascribed to a pronounced spin–orbit coupling for the $^5\text{T}_{2g}$ ground state of the Fe(II) ion in the octahedral environment.

Introduction

Layered solids consisting of alternating inorganic and organic layers are interesting materials for several reasons. They in fact can be used as ion exchangers, catalysts, and hosts in intercalation compounds and have also provided interesting examples of low-dimensional magnetic materials.^{1,2} Typical layered materials are the “intercalation”³ and “molecular composite”⁴ compounds. In contrast with intercalation compounds, which can exist both with and without organic molecules between

layers of the lattice, in molecular composite solids, the organic groups are covalently or ionically bound to the inorganic layers. Two well-known examples of the latter type of solids are represented by the layered perovskite halides of general formula $(\text{RNH}_3)_2[\text{MX}_4]$ ⁵ ($\text{R} = \text{alkyl}$ or aryl group, $\text{M} = \text{divalent metal ion}$, $\text{X} = \text{Cl, Br, I}$) and by the metal organophosphonates.⁶ An important feature shown by such materials is the possibility of combining physical properties typical of the inorganic solid state, like *ferromagnetism*, *luminescence*, *semiconducting behavior*, with properties easily found in the organic solid state, like *mesomorphism*, *nonlinear optics*, *polymerization*, *plastic mechanical properties*, etc. For the above-mentioned reasons, we have undertaken a study of some transition metal(II) organophosphonates. This widespread group of salts has the general formula $\text{M}_2[\text{O}_3\text{P}-(\text{CH}_2)_n-\text{PO}_3]\cdot 2\text{H}_2\text{O}$ ⁶ and $\text{M}[\text{C}_n\text{H}_{2n+1}\text{PO}_3]\cdot$

(1) (a) Alberti, G. In *Comprehensive Supramolecular Chemistry*; Lehn, J. M., Ed.; Pergamon Press: New York, 1996; Vol. 7. (b) Clearfield, A. In *New Developments in Ion Exchange Materials*; Abe, M., Kataoka, T., Suzuki, T., Eds.; Kodansha Ltd.: Tokyo, 1991. (c) Cao, G.; Hong, H.; Mallouck, T. E. *Acc. Chem. Res.* **1992**, *25*, 420.

(2) Navarro, R. In *Magnetic Properties of Layered Transition Metal Compounds*; De Jongh, L. J., Ed.; Kluwer: Dordrecht, The Netherlands, 1990.

(3) O'Hare, D. In *Inorganic Materials*; Bruce D. W., O'Hare, D., Eds.; John-Wiley & Sons: New York, 1992.

(4) Day P. *Philos. Trans. R. Soc. London.* **1985**, *A314*, 145.

(5) Bellitto, C.; Day, P. In *Comprehensive Supramolecular Chemistry*; Lehn, J. M., Ed.; Pergamon Press: New York, 1996; Vol. 7, pp 293–312.

(6) Clearfield, A. *Prog. Inorg. Chem.* **1998**, *47*, 371.

H_2O^7 ($M = \text{divalent metal ion}$), and in the most usual crystal structure, the metal ions are bridged by the oxygens of the phosphonate ligands to form sheets separated from one another by the organic substituents of the ligands. A recent study of the magnetic properties of $\text{Mn}[\text{C}_n\text{H}_{2n+1}\text{PO}_3] \cdot \text{H}_2\text{O}$ ⁸ has shown that the compounds order antiferromagnetically at low temperatures. Below the ordering temperature, T_N , the equilibrium distribution of moments is not collinear but canted from the magnetic easy axis, giving rise to a spontaneous magnetization, as demonstrated recently by Talham et al. using an antiferromagnetic resonance (AFMR) technique in Mn(II) phosphonates.⁹ This phenomenon is known as *canted antiferromagnetism* or *weak ferromagnetism*, and it has been observed for the first time in $\alpha\text{-Fe}_2\text{O}_3$.¹⁰ “Weak” ferromagnetic solids represent the third kind of magnetic solids, with a finite zero-field magnetization, the other two examples being ferromagnets and ferrimagnets. Moreover, this type of magnetic ordered state has been observed recently in molecular-based solids and in particular in three metal(II) organophosphonates (i.e., in $\text{Fe}[\text{C}_2\text{H}_5\text{PO}_3] \cdot \text{H}_2\text{O}$,¹¹ $\text{Cr}[\text{CH}_3\text{PO}_3] \cdot \text{H}_2\text{O}$,¹² and $\text{Fe}_2[\text{O}_3\text{P}-(\text{CH}_2)_2-\text{PO}_3] \cdot 2\text{H}_2\text{O}$.¹³

This paper deals with the synthesis, chemical and structural characterization, and a magnetic study of Fe(II) phenylphosphonate. The room-temperature crystal structure of the compound was determined from X-ray powder diffraction data and refined by the Rietveld method.

Experimental Section

Materials and Methods. Phenylphosphonic acid, $\text{C}_6\text{H}_5\text{PO}_3\text{H}_2$, was of analytical grade (Aldrich Chemical Co.) and was used without further purification. HPLC water was used as solvent. All reactions involving the Fe(II) ion were carried out under an inert atmosphere by using the usual Schlenk techniques. Water was purged with N_2 gas prior to use. Elemental analyses were performed by Malissa and Reuter Mikroanalytische Laboratorien, Elbach, Germany. Thermogravimetric analysis (TGA) data were collected in flowing dry N_2 at a rate of $5^\circ\text{C}/\text{min}$ on a Stanton-Redcroft STA-781 thermoanalyzer. The IR absorption spectra were obtained by using a Perkin-Elmer 621 spectrophotometer by the KBr pellet method. Static magnetic susceptibility measurements were performed by using a Quantum Design MPMS5 superconducting quantum interference device (SQUID) susceptometer in fields up to 5 T. A cellulose capsule was filled with freshly prepared polycrystalline sample and placed inside in a polyethylene straw. All the experimental data were corrected for the core magnetization using Pascal's constants.

Synthesis of $\text{Fe}[\text{C}_6\text{H}_5\text{PO}_3] \cdot \text{H}_2\text{O}$. This compound was prepared by a slightly different procedure from that reported previously by us¹³ because of the partial insolubility of the phenylphosphonate ligand in

water. First, a solution containing the ammonium phenylphosphonate was prepared by adding ~ 7 mL of a 30% ammonia solution to a mixture of the acid (10 g, 63.25 mmol) and water (50 mL) until the solution becomes clear and the pH = 7. The resulting colorless solution was degassed and then added to a solution of $\text{FeSO}_4 \cdot 7\text{H}_2\text{O}$ (7 g, 25.18 mmol) dissolved in 35 mL of water. The white-gray microcrystalline precipitate formed immediately, which was kept under stirring for a few minutes. The precipitate was then washed with water and acetone and then dried under vacuum. The compound is stable in air. The composition of the material was checked by elemental analyses and by TGA measurements.

Anal. Calcd for $\text{Fe}[\text{C}_6\text{H}_5\text{PO}_3] \cdot \text{H}_2\text{O}$: Fe, 24.28; C, 31.34; H, 3.07; P, 13.47; O, 20.87. Found: Fe, 23.80; C, 30.95; H, 3.13; P, 12.37.

X-ray Data Collection. Room-temperature X-ray powder diffraction data were recorded on a Seifert XRD-3000 diffractometer, with a curved graphite single-crystal monochromator [$\lambda(\text{Cu K}\alpha_1, \text{K}\alpha_2) = 1.5406/1.5444 \text{ \AA}$] and a position-sensitive detector operating in constant mode. The data were collected with a step size of 0.02° , 2θ , and at count time of 4s per step of $0.2^\circ \text{ min}^{-1}$ over the range $4^\circ < 2\theta < 80^\circ$. The sample was mounted on a flat plate, giving rise to a strongly preferred orientation. The diffractometer zero point was determined from an external Si standard. The powder diffraction pattern was indexed by using a Seifert indexing program in the orthorhombic system with the following unit-cell parameters: $a = 5.67 \text{ \AA}$, $b = 14.45 \text{ \AA}$, $c = 4.89 \text{ \AA}$. The unit cell parameters suggest that the compound is isomorphous to $\text{Mg}[\text{C}_6\text{H}_5\text{PO}_3] \cdot \text{H}_2\text{O}$ ¹⁴ and $\text{Cd}[\text{C}_6\text{H}_5\text{PO}_3] \cdot \text{H}_2\text{O}$.^{7b} The systematic absences were consistent with the space group $Pmn2_1$.

Structure Solution and Refinement. The structure determination of the title compound was carried out by the EXPO program.¹⁴ EXPO first decomposed the X-ray powder pattern by the Le Bail method,¹⁵ using information on the cell parameters, the space group, and the wavelength used. The data for the profile fitting were evaluated in the angular range $4^\circ - 70^\circ 2\theta$ because of the strong intensity decay at large 2θ values. An amount of 123 extracted integrated intensities (53 independent observations because of the reflection overlapping) were used in the direct methods procedures to solve the crystal structure. The E-map corresponding to the best figure of merit (CFOM = 0.999) was selected and optimized by a least-squares routine where the ratio “number of independent observations/number of parameters” to refine was small (i.e., ~ 0.9). The parameter multiplying the full width at half-maximum, fwhm, of each reflection was modified (i.e., 0.3 instead of 0.7) to change the overlapping criterion for obtaining a larger number of independent groups of overlapping reflections used in the least squares routine. The ratio became 1.5. At the end, the optimized Fourier map allowed the positioning of six atoms (1 Fe, 1 P, 3 O, 1 C) out of the total of 13 atoms in the asymmetric unit. $\text{Fe}[\text{C}_6\text{H}_5\text{PO}_3] \cdot \text{H}_2\text{O}$ was found to be isomorphous with the Mn(II), Zn(II), and Cd(II) analogues. Starting with the atomic positions found by EXPO, the other unlocated atoms were constructed by restraining them to the geometrical configuration of the corresponding Cd salt. Then the refinement of the title compound was carried out with the PC version of the crystal structure analysis package GSAS.¹⁶ Powder diffraction patterns were calculated for this model in the orthorhombic space group $Pmn2_1$ and by using the unit cell parameters refined by a least-squares procedures described above. Data were evaluated in the $4 - 65^\circ$ angular range. By use of the utility program CONVERT,¹⁷ the raw data were transferred to the GSAS program package for full profile refinement. Initially, the scale factor, the lattice parameters, the background coefficients, and the peak shape parameters were refined. Atomic positions were refined with soft constraints for the ligand by fixing the P–C bond and the P–O distances at ~ 1.80 and $\sim 1.50 \text{ \AA}$, respectively. The refinement in the space group $Pmn2_1$ showed that the phenyl groups are disordered in two orientations. The disorder was assumed to be due to the rotation

- (7) (a) Cao, G.; Lee, H.; Lynch, V. M.; Mallouk, T. E. *Inorg. Chem.* **1988**, *27*, 2781. (b) Cao, G.; Lee, H.; Lynch, V. M.; Yacullo, L. M. *Chem. Mater.* **1993**, *5*, 1000. (c) Martin, K. J.; Squattrito, P. J.; Clearfield, A. *Inorg. Chim. Acta* **1989**, *155*, 7.
- (8) (a) Carling, S. G.; Day, P.; Visser, D.; Deportes, J. J. *Appl. Phys.* **1991**, *69*, 6016. (b) Carling, S. G.; Day, P.; Visser, D.; Kremer, R. K. *J. Solid State Chem.* **1993**, *106*, 111.
- (9) (a) Fanucci, G. E.; Krzysiek, J.; Meisel, M. W.; Brunel, L. C.; Talham, D. L. *J. Am. Chem. Soc.* **1998**, *120*, 5469. (b) Seip, C. T.; Granroth, G. E.; Meisel, M. W.; Talham D. L. *J. Am. Chem. Soc.* **1997**, *119*, 7084.
- (10) Carlin, R. L. *Magnetochemistry*; Springer-Verlag: Berlin, 1986; p 149. (b) Moriya, T. *Phys. Rev.* **1960**, *120*, 91. (c) Shull, C. G.; Strasser, W. A.; Wollan E. O. *Phys. Rev.* **1951**, *83*, 333.
- (11) (a) Bujoli, B.; Pena, O.; Palvadeau, P.; Le Bideau, J.; Payen, C.; Rouxel, J. *Chem. Mater.* **1993**, *5*, 583. (b) Le Bideau, J.; Payen, C.; Bujoli, B.; Palvadeau, P.; Rouxel, J. *J. Magn. Magn. Mater.* **1995**, *140*, 1719.
- (12) (a) Bellitto, C.; Federici, F.; Ibrahim, S. A. *J. Chem. Soc., Chem. Commun.* **1996**, 759. (b) Bellitto, C.; Federici, F.; Ibrahim, S. A. *Chem. Mater.* **1998**, *10*, 1076.
- (13) Bellitto, C.; Federici, F.; Ibrahim, S. A.; Mahmoud, M. R. *1998 MRS Fall Meetings Proceedings*; Materials Research Society: Warrendale, PA, 1999; 547, pp 487.

- (14) Altomare, A.; Burla, M. C.; Camalli, M.; Carrozzini, B.; Cascarano, G.; Giacovazzo, C.; Guagliardi, A.; Moliterni, A. G. G.; Polidori, G.; Rizzi, R. *J. Appl. Crystallogr.* **1999**, *32*, 339.
- (15) Le Bail, A.; Duray, H.; Fourquet, J. L. *Mater. Res. Bull.* **1988**, *23*, 447.
- (16) GSAS: *Generalized Structure Analysis System*; Larson, A., von Dreele R. B., Eds.; Los Alamos National Laboratory: Los Alamos, NM, 1985.
- (17) Drogue, N. *CONVERT*, version 3.02; University of Bucharest: Bucharest, Romania, 1988.

Table 1. Crystallographic Data for $\text{Fe}[\text{C}_6\text{H}_5\text{PO}_3]\cdot\text{H}_2\text{O}$

formula	$\text{FeO}_4\text{PC}_6\text{H}_7$
fw	229.94
space group	$Pmn2_1$ (no.31)
a (Å)	5.668(8)
b (Å)	14.453(2)
c (Å)	4.893(7)
cell vol (Å ³)	400.8(2)
Z	2
T (°C)	room temp
λ (Cu $K\alpha_1$, $K\alpha_2$) (Å)	1.5406/1.5444
d_c (g/cm ³)	1.905
pattern range (2θ , deg)	4–65
no. of refined parameters	18
R_p^a	0.134
R_{pw}^a	0.174

^a See ref 16 for definitions.

Table 2. Bond Lengths (Å) and Angles (deg) for the Non-hydrogen Atoms for $\text{Fe}[\text{C}_6\text{H}_5\text{PO}_3]\cdot\text{H}_2\text{O}$

atom number			bond 1–2	angle 1–2–3
1	2	3		
O(1)	Fe	O(2a)	1.951(1)	90.4(1)
O(1)	Fe	O(2d)	94.3(1)	
O(3)	Fe	O(1)	2.285(3)	82.5(1)
O(2)	Fe	O(2c)	2.037(1)	114.1(1)
O(2)	Fe	O(2e)	2.412(1)	94.8(1)
O(2'')	Fe	O(2b)	2.412(1)	55.6(1)
O(2)	Fe	O(3)	58.4(1)	
O(2')	Fe	O(3)	151.4(1)	
O(1)	P	O(2)	1.487(3)	101.3(1)
O(2)	P	O(2')	97.7	
O(2)	P	C(1)	1.494(1)	117.9
C(1)	P	O(1)	1.794(1)	117.3(1)
C(2)	C(1)	P	1.439(1)	123.3(1)
C(2)	C(1)	C(2)	113.2(1)	
C(3)	C(2)	C(1)	1.341(1)	121.7(1)
C(4)	C(3)	C(2)	1.393(1)	124.4(1)
C(3)	C(4)	C(3)	114.0(1)	
C(4A)	C(3A)	C(1)	1.397(1)	122.1(1)
C(6A)	C(1)	C(3A)	1.366(1)	116.5(1)

of the phenyl group around the P–C bond while the positions of C1 and C4 were left unaffected by the disorder. The refinement with site occupancy factors of the atoms in the two orientations fixed at 0.5 resulted in $R_p = 13.4\%$, $R_{pw} = 17.4\%$, and $\chi^2 = 0.6$. In the last stage of the refinement the atomic isotropic thermal parameters were also refined. A correction was made for the preferred orientation [010] by using the March–Dollase method in the GSAS suit of programs.¹⁸ Crystallographic and experimental parameters are given in Table 1 and bond parameters in Table 2. The final Rietveld refinement difference plot is shown in Figure 1.

Results

$\text{Fe}[\text{C}_6\text{H}_5\text{PO}_3]\cdot\text{H}_2\text{O}$ was prepared by using a method different from that described in the literature for the only reported iron(II) ethylphosphonate,¹¹ by starting from $[\text{FeSO}_4]\cdot 7\text{H}_2\text{O}$ in water in the presence of ammonium phenylphosphonate at temperatures slightly above 70 °C under inert atmosphere. Under these conditions the deprotonated acid is present in solution, thus favoring the complexation and the precipitation of a solid. The compound was isolated as a light-gray, air-stable microcrystalline solid. The TGA results for $\text{Fe}[\text{C}_6\text{H}_5\text{PO}_3]\cdot\text{H}_2\text{O}$ are reported in Figure 2 and show that the first loss starting at 30 °C is completed at 180 °C (6.21%) and that it corresponds roughly to one molecule of water. After dehydration from 320 to 500 °C, there is a loss of 28.7%, which corresponds to the decomposition of the ligand.

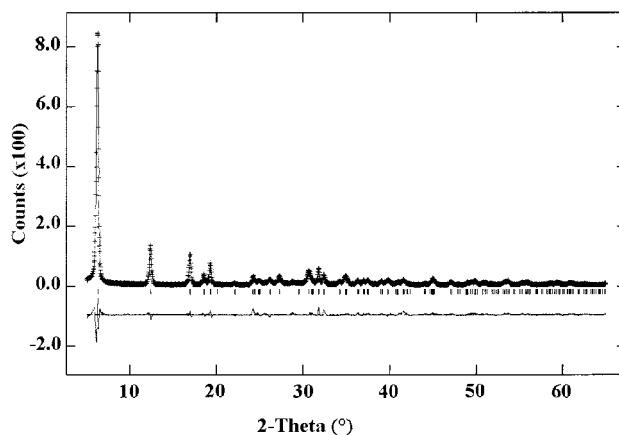


Figure 1. Observed (+) and calculated (–) powder X-ray diffraction profiles for the Rietveld refinement of $\text{Fe}[\text{C}_6\text{H}_5\text{PO}_3]\cdot\text{H}_2\text{O}$. The bottom curve is the difference plot on the same scale intensity. The tic marks are calculated 2θ angles for Bragg peaks.

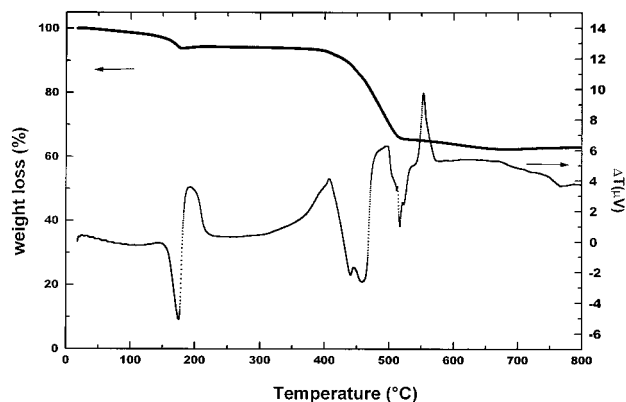


Figure 2. TGA and differential scanning calorimetry (DSC) curves of $\text{Fe}[\text{C}_6\text{H}_5\text{PO}_3]\cdot\text{H}_2\text{O}$.

Crystal Structure of $\text{Fe}[\text{C}_6\text{H}_5\text{PO}_3]\cdot\text{H}_2\text{O}$. $\text{Fe}[\text{C}_6\text{H}_5\text{PO}_3]\cdot\text{H}_2\text{O}$ crystallizes in the orthorhombic system $Pmn2_1$ with the following unit cell parameters: $a = 5.668(8)$ Å, $b = 14.453(2)$ Å, $c = 4.893(7)$ Å, $Z = 2$. The structure is isomorphous and isostructural with that of Mn, Zn, and Cd phenylphosphonates.⁷ The unit cell packing of the compound along the c axis is shown in Figure 3, and the projection along the b axis is presented in Figure 4. The iron atoms are six-coordinated by five oxygens of the phosphonate groups (O1,O2) and one from the water molecule (O3). Since the compound contains only one phosphonate per metal ion, all the phosphonate oxygen atoms take part in metal binding and two oxygens (O2) chelate the metal ion and at the same time bridge adjacent metal ions in the same row. Oxygen O1 of the phosphonate lying in the mirror plane bonds to only one Fe atom, and it is located trans to the oxygen of the water molecule. The octahedron is distorted, and one of the cis O–Fe–O angles is small (56°), while the others range between 83° and 116° . Iron atoms are linked along the a axis by the third oxygen of the phosphonate, O2, to form a kinked or crenelated (ac) layer. The P–C bond and the plane containing the phenyl group are nearly perpendicular to the inorganic network between layers, and the organic group is disordered between two orientations perpendicular to each other within a single layer. The layers are then translationally related along the b axis. Further, the disorder occurs in the b direction through stacking disorder or twinning.

Optical Properties. The IR spectrum of $\text{Fe}[\text{C}_6\text{H}_5\text{PO}_3]\cdot\text{H}_2\text{O}$ is reported in Figure 5. It features two intense and sharp bands,

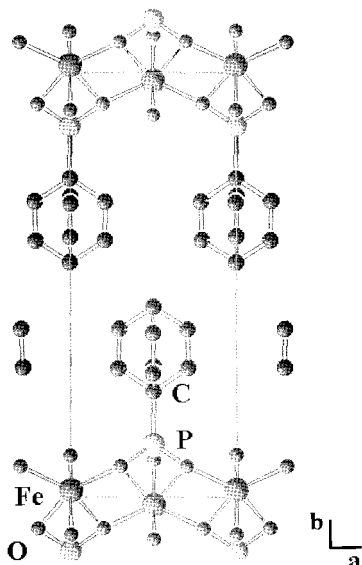


Figure 3. Unit-cell packing of $\text{Fe}[\text{C}_6\text{H}_5\text{PO}_3]\cdot\text{H}_2\text{O}$ viewed along the c axis, showing the arrangement of the phenyl groups in the lattice.

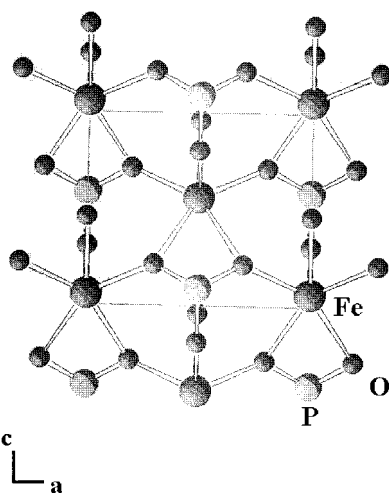


Figure 4. Structure of $\text{Fe}[\text{C}_6\text{H}_5\text{PO}_3]\cdot\text{H}_2\text{O}$ viewed along the b axis. Phenyl groups are omitted for clarity.

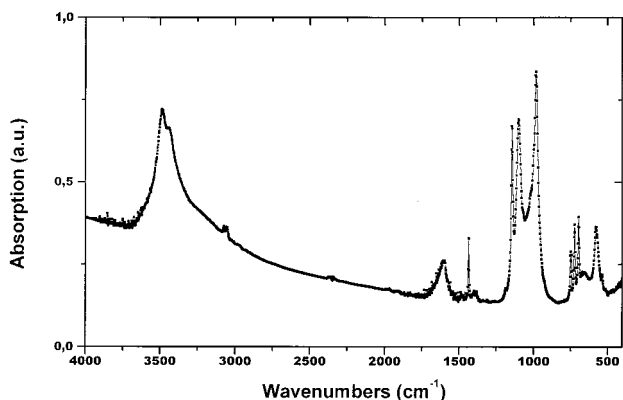


Figure 5. Absorption FTIR spectrum of $\text{Fe}[\text{C}_6\text{H}_5\text{PO}_3]\cdot\text{H}_2\text{O}$ in the KBr region.

centered at about 3420 and 3470 cm^{-1} and one at 1604 cm^{-1} (m), assigned as O–H stretching vibrations and H–O–H bending vibration of water molecules, respectively. The strong and sharp nature of these bands indicates that the water is coordinated to the metal ion, in agreement with TGA and structural results. The sharp bands at 3074 and 3054 cm^{-1} are

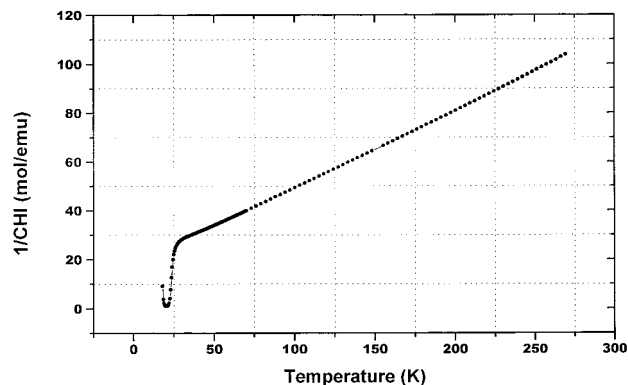


Figure 6. $1/\chi$ vs T plots of $\text{Fe}[\text{C}_6\text{H}_5\text{PO}_3]\cdot\text{H}_2\text{O}$ in the temperature range 20 – 270 K .

due to the C–H stretching vibrations of the phenyl group. The C–C skeletal vibration of the phenyl group is observed at 1438 cm^{-1} , while the four bands in the range 1200 – 970 cm^{-1} can be assigned as $[\text{PO}_3]$ group stretching vibrations. The complete conversion of the acid to the Fe(II) salt is demonstrated by the absence of O–H stretching vibrations of the hydrogen phosphonate group, usually observed at ~ 2900 and 2300 cm^{-1} .¹⁹ The optical spectrum in the NIR–visible region is similar to that of $[\text{Fe}(\text{H}_2\text{O})_6]^{2+}$, where only the spin-allowed ${}^5\text{T}_{2g} \rightarrow {}^5\text{E}_g$ is expected. The absorption spectra consist of two broad peaks centered at 9300 cm^{-1} and the other, even broader, at 6250 cm^{-1} , probably because of a low-symmetry ligand field component, which lifts the two-orbital degeneracy of the ${}^5\text{E}_g$ term.

Magnetic Properties. (a) Paramagnetic Region. As a background to looking in more detail at the magnetic properties of the title compound, magnetic susceptibility measurements were performed on a polycrystalline sample in the paramagnetic region at temperatures from 80 to 270 K and in an applied field of 50 mT . The inverse of molar magnetic susceptibility, $1/\chi_M$, as a function of the temperature, T , in the range 20 – 270 K , is shown in Figure 6. Above 80 K , the magnetic behavior is linear according to the Curie–Weiss law, and the Curie constant, C , is $3.15\text{ emu K mol}^{-1}$, as fitted to the high-temperature susceptibility data by using the equation $\chi = C/(T - \theta)$. This corresponds to an effective magnetic moment of $5.0\ \mu_B$, consistent with the presence of Fe(II) in a d^6 high-spin electronic configuration. This value is slightly higher than that expected for the spin-only moment (i.e., $4.9\ \mu_B$). The ${}^5\text{D}$ ($L = 2$) free-ion state of the Fe(II) ion has an orbital degeneracy, and in a cubic ligand field, the ground state is the ${}^5\text{T}_{2g}$ ground state, with the lowest spin-orbit state with $J = 1$.²⁰ An introduction of a distortion in the $[\text{FeO}_6]$ site by the ligands causes a further splitting of the $J = 1$ state, and the resulting ground state can be either a singlet, $M_J = 0$, or doublet, $M_J = \pm 1$. Because the energy separation between the spin-orbit components in Fe(II) is about 200 cm^{-1} , we expect an orbital contribution to the Fe(II) moment, which could explain the observed difference. The Weiss constant (i.e., $\theta = -56\text{ K}$) is negative and high in value, thus indicating strong antiferromagnetic near-neighbor exchange interactions between the adjacent iron(II) ions.

(b) Low-Temperature Magnetic Behavior. Below 100 K , $\chi_M T$ slightly decreases, thus indicating antiferromagnetic interaction between Fe(II) ions, and then at about 25 K , it rises to a maximum at $T \cong 21\text{ K}$ and then decreases again. The peak

(19) Cabeza, A.; Aranda, M. G. A.; Bruque, S.; Poojary, D. M.; Clearfield, A. *Mater. Res. Bull.* **1998**, *33*, 1265.

(20) Figgis, B. N. *Introduction to Ligand Fields*; Interscience: London, 1966; p 289.

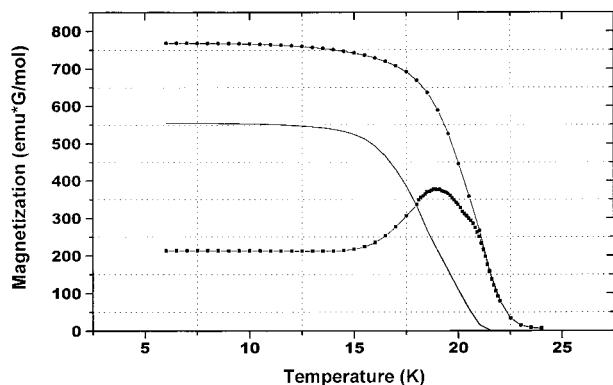


Figure 7. Temperature dependence of the ZFCM (■) and FCM (●) magnetization of $\text{Fe}[\text{C}_6\text{H}_5\text{PO}_3]\cdot\text{H}_2\text{O}$ below 25 K. The full line is the remnant magnetization, as obtained from the difference of the FCM and ZFCM plots.

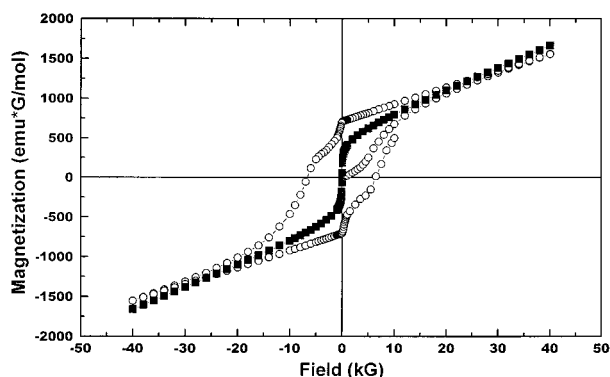


Figure 8. Hysteresis loops of $\text{Fe}[\text{C}_6\text{H}_5\text{PO}_3]\cdot\text{H}_2\text{O}$ measured at $T = 10$ K (○) and at $T = 21$ K (■).

can be associated with a three-dimensional antiferromagnetic ordering. Field-cooled (FCM) and the zero-field-cooled (ZFCM) magnetizations in the 6–25 K temperature range were also measured, and the plot is shown in Figure 7. The ZFCM, obtained on cooling the sample in zero field and then warming it in the field of 100 G, shows a broad peak centered at $T \approx 21$ K. The FCM, obtained on cooling the sample within the same field of 100 G, shows a rapid increase at $T = 23$ K, and then it starts to be constant at $T \approx 13$ K down to the lowest measured $T = 6$ K. The difference between FCM and ZFCM represents the remnant magnetization, induced by cooling within a field below 24 K and switching off the field. The remnant magnetization disappears upon warming to $T = 21.5$ K, and this temperature is taken as the critical temperature, T_N . Isothermal magnetization as a function of magnetic field was measured at $T = 10$ K, a temperature well below the critical temperature. It reaches the value of ~ 1700 emu G mol $^{-1}$ at 4 T, and this value is $\sim 7\%$ of that expected for an $S = 2$ system. Hysteresis loops at $T = 10$ K and at $T = 21$ K are shown in Figure 8. The plot at $T = 10$ K shows that the values of the coercive field, H_c , and of the remnant magnetization, M_r , are 6400 G and 740 emu G mol $^{-1}$, respectively. The hysteresis loop, measured near the critical temperature (i.e., $T = 21$ K), shows that the magnetization is the sum of two contributions $M = M_{nc} + \chi_{AFM}H$, where M_{nc} is the uncompensated (weak ferromagnetic) moment and χ_{AFM} is the antiferromagnetic susceptibility. M_{nc} was determined from the extrapolation to zero field of the linear part of the magnetization curve at high applied magnetic fields, and χ_{AFM} was determined as its slope. The values were found to be 550 emu G mol $^{-1}$ and 0.029 emu mol $^{-1}$, respectively. Hysteresis phenomena disappear at temperatures above T_N , where the

isothermal magnetization vs field plot is linear. These results indicate definitely that the magnetic behavior of the title compound is characteristic of a “weak” ferromagnet or “canted” antiferromagnet. The magnetic parameters of $\text{Fe}[\text{C}_6\text{H}_5\text{PO}_3]\cdot\text{H}_2\text{O}$ are reported in Table 3, together with those of the analogues taken from literature. The purely inorganic $(\text{NH}_4)\text{Fe}^{\text{II}}\text{PO}_4\cdot\text{H}_2\text{O}$ has been included because it possess the same metal–oxygen–phosphorus layer and also because it is a “canted” antiferromagnet. The NH_4^+ ion lies in the interlayer region, and the organic phosphonic groups are replaced by the phosphate oxygen.²¹ In this series the inorganic Fe(II) phosphate, ($T_N = 24.0$ K) and the two known Fe(II) organophosphonates ($T_N = 24$ – 25 K) show the same values for the critical temperature, while for the title compound ($T_N = 21.5$ K) the observed critical temperature is slightly lower.

Conclusions

Molecule-based “weak” ferromagnets are uncommon. In this work, we have reported on the synthesis and the chemical, structural, and magnetic characterization of a new, “weak ferromagnet” of formula $\text{Fe}[\text{C}_6\text{H}_5\text{PO}_3]\cdot\text{H}_2\text{O}$. The synthetic method is reliable for preparing pure Fe(II) phosphonates.^{13,22} The crystal structure was solved by Rietveld refinement of X-ray powder data, and the compound has been found to have a lamellar structure made of alternating inorganic and organic layers. The former is made of Fe(II) octahedrally coordinated to the oxygens of the phosphonate ligand and to the water molecule, producing a cross-link Fe–O network. The phenyl groups are located above and below these sheets, making van der Waals contacts between the organic bilayers. The plane containing the organic group is nearly perpendicular to the plane of the inorganic network, but it is disordered between two orientations. The structural data are not reliable enough to provide details of the site symmetry of the metal ion. The compound orders antiferromagnetically at $T_N = 21.5$ K, and the antiferromagnetism arises from interactions between nearest-neighbor ions that take place via two different 180° Fe–O–Fe superexchange paths. The value of the $|T_c/\theta|$ ratio is ~ 0.4 (see Table 3), and this experimental finding is consistent with the layered structure. Molecular field predicts $|T_c/\theta| = 1$, but large deviations are expected for low-dimensional magnets because of the short-range correlations above the critical temperature T_N .² Below T_N , the observed weak ferromagnetism is due to the spin canting.¹⁰ In this situation the local spins in the ordered magnetic state are not perfectly antiparallel, which results in an uncompensated resultant moment in one direction. There are two mechanisms for producing the canted spin structure in these solids: single-ion magnetic anisotropy^{10a,23} and the so-called antisymmetric Dzyaloshinsky–Moriya (DM) exchange coupling,²⁴ which may occur between neighboring centers and compete with isotropic Heisenberg antiferromagnetic exchange. The first mechanism operates when there are two equivalent sites of magnetic ions, but the directions of their anisotropy axes are different. The DM mechanism acts to cant the spins because the coupling energy is minimized when the two spins are perpendicular to each other. This coupling operates in addition to isotropic Heisenberg exchange, and it depends on the symmetry of the crystal (the magnetic ions in the unit

(21) (a) Carling, S. G.; Day, P.; Visser, D. *Inorg. Chem.* **1995**, *34*, 3917.

(b) Greedan, J. E.; Reubeunbauer, K.; Birchall, T.; Ehlert, M.; Corbin, D. R.; Subramanian, M. A. *J. Solid State Chem.* **1988**, *77*, 376.

(22) See ref 6, p 469.

(23) Moriya, T. *Phys. Rev.* **1960**, *117*, 635.

(24) Dzyaloshinsky, I. *J. Phys. Chem. Solids* **1958**, *4*, 241.

Table 3. Magnetic Parameters of Fe(II) Phosphonates

compd	T_N (K)	θ (K)	T_N/θ	space group	a (Å)	b (Å)	c (Å)	β (deg)	ref
(NH ₄)FePO ₄ ·H ₂ O	24.0	−65	0.37	<i>Pmn</i> 2 ₁	5.6656(1)	8.8213(2)	4.8314(1)		21
Fe(C ₂ H ₅ PO ₃)H ₂ O	24.5	−43	0.57	<i>P1n</i> 1	5.744(3)	10.33(1)	4.856(8)	91.0(1)	11a
Fe(C ₆ H ₅ PO ₃)H ₂ O	21.5	−56	0.38	<i>Pmn</i> 2 ₁	5.668(8)	14.453(2)	4.893(7)		this work
Fe ₂ [O ₃ P(CH ₂) ₂ PO ₃]·2H ₂ O	24.0	−55	0.44		5.67	15.23	4.82		13

cell cannot be related by a center of symmetry). Now in Fe-[C₆H₅PO₃]·H₂O, the symmetry of the space group is *Pmn*2₁, and it is low enough to allow the Dzyaloshinsky–Moriya exchange coupling. The antisymmetric exchange could then be responsible for the spontaneous magnetization observed in this compound. This mechanism has been suggested to operate in Mn(II) alkylphosphonates.^{8b} But the Fe(II) ion has a single-ion anisotropy due to the spin–orbit coupling, so this contribution must also be taken into account. An indication of the latter comes from the observed very high value of the coercive field, which is uncommon for a molecular material. Finally, the critical temperatures, observed in the iron(II) phosphonate series, appear to depend little on the interlayer spacing, similar to that observed in the manganese analogues.⁹

Acknowledgment. We acknowledge support from Consiglio Nazionale delle Ricerche (Italy) and the Academy of Scientific Research and Technology (Egypt) in the framework of their Scientific Agreement. One of the authors (C.B.) thanks Mr. P. Filaci, Mrs. C. Riccucci, and Mr. C. Veroli for technical assistance and one of the reviewers for helpful criticism. The Royal Institution of Great Britain, London, is also acknowledged for allowing one of the authors (C.B.) to repeat magnetic experiments using their SQUID Quantum Design MPMS7.

Supporting Information Available: Table S1 providing a complete listing of atomic parameters and isotropic thermal displacement parameters for Fe[C₆H₅PO₃]·H₂O. This material is available free of charge via the Internet at <http://pubs.acs.org>.

IC9914995